Precoding for Point-to-Multipoint Transmission over MIMO ISI Channels

Robert F.H. Fischer, Clemens Stierstorfer, Johannes B. Huber

Lehrstuhl für Informationsübertragung, Universität Erlangen, Cauerstraße 7, 91058 Erlangen, Germany, fischer@LNT.de

***Abstract*— Tomlinson-Harashima type precoding for point-to-multipoint transmission over linear dispersive channels which suffer from intersymbol interference and multiuser interference is reviewed. The tasks of the matrix filters at the joint transmitter, their calculation by spectral factorization, and the necessity of an optimized processing order are discussed. The performance of precoding is covered by numerical simulations.**

I. Introduction

Over the last years, transmission of multiple data streams in parallel, e.g., by using antenna arrays in transmitter and receiver, creating a multiple-input/multiple-output (MIMO) channel, has become very popular. If, additionally, the channels suffer from intersymbol interference (ISI) (MIMO ISI channel), the received signals are affected by both, ISI and multiuser interference (MUI).

In this paper, we study point-to-multipoint transmission, i.e., transmission from a central transmitter (using multiple transmit antennas) to distributed (decentralized) receivers (each having one antenna). For the flat fading case, it has been recognized, e.g., [10], [8], [6], [2], that Tomlinson-Harashima type precoding [16], [12], initially introduced for ISI channels, is also an attractive scheme for nonlinear preequalization of MIMO channels. Here we show the application of precoding to point-to-multipoint transmission over MIMO ISI channels.

After explaining the channel model (Section II), we derive the optimum matrix filters for joint preprocessing at the transmitter and discuss the role of an optimized processing order (Sections III and IV). Results from numerical simulations are given in Section V.

II. Channel Model

We assume transmission from a central transmitter with N transmit antennas over an ISI producing channel to $K \leq N$ receivers, each equipped with one antenna (MIMO ISI channel).[1] To each of the receivers T-spaced data symbols $a_\kappa[k]$, $k \in \mathbb{Z}$, $\kappa = 1, \ldots, K$, taken from a signal constellation $\mathcal{A}$ (with $\sigma_a^2 \overset{\text{def}}{=} \mathrm{E}\{|a_\kappa[k]|^2\}$, $\forall\kappa$) and combined into the vector[2] $\boldsymbol{a}[k] = [a_1[k], \ldots, a_K[k]]^{\mathsf{T}}$ have to be transmitted.

The MIMO ISI channel (equivalent complex baseband notation, we restrict ourselves to linear time-invariant dispersive channels) is characterized by the set of continuous-time impulse responses $h_{\mathrm{C},\kappa,\nu}(t) \circ\!\!-\!\!\bullet\, H_{\mathrm{C},\kappa,\nu}(f)$ from transmit antenna ν to receive antenna κ, and we define the channel matrix $\boldsymbol{H}_{\mathrm{C}}(f) \overset{\text{def}}{=} [\, H_{\mathrm{C},\kappa,\nu}(f)\,]$. It it reasonable to assume the additive Gaussian noise $n_\kappa(t)$ at the receive antennas (arranged into the vector $\boldsymbol{n}(t)$) to be spatially and temporally white, each with noise power spectral density N_0.

By transferring the optimal receiver-side processing for MIMO ISI channels [4], [5] (see also the general principle in [3]) to the transmitter, we end up with the transmission scheme shown in Fig. 1. Given the symbols $a_\kappa[k]$, via discrete-time joint processing channel symbols $x_\kappa[k]$ are generated, from which continuous-time signals are obtained through (individual) pulse shaping by the continuous-time transmit filter with transfer function $T \cdot H_{\mathrm{T}}(f) \bullet\!\!-\!\!\circ\, T \cdot h_{\mathrm{T}}(t)$ (assumed to have square-root Nyquist characteristics). Then, the matrix matched filter is applied to generate the continuous-time antenna signals. At the receiver side, only matched filtering by $H_{\mathrm{T}}^*(f)$ and T-spaced sampling is performed.

For the subsequent discussion, a discrete-time channel model, including transmit filters, matrix matched filtering with respect to the channel at the transmitter and individual matched filtering with respect to the pulse shape and T-spaced sampling at the receiver, can be put up, cf. Fig. 1. The $K \times K$ discrete-time matrix channel $\boldsymbol{H}_{\mathrm{o}}(z)$, evaluated on the unit circle, calculates to

$$\boldsymbol{H}_{\mathrm{o}}(\mathrm{e}^{\mathrm{j}2\pi fT}) = \sum_{l=-\infty}^{+\infty} H_{\mathrm{T}}^*(f+\tfrac{l}{T})\boldsymbol{H}_{\mathrm{C}}(f+\tfrac{l}{T}) \cdot \boldsymbol{H}_{\mathrm{C}}^{\mathsf{H}}(f+\tfrac{l}{T}) H_{\mathrm{T}}(f+\tfrac{l}{T})\,. \tag{1}$$

Due to square-root Nyquist characteristic of the transmit filters, the autocorrelation matrix of the additive noise $\boldsymbol{n}_{\mathrm{o}}[k]$ reads $\boldsymbol{\Phi}_{n_{\mathrm{o}}n_{\mathrm{o}}}[\kappa] \overset{\text{def}}{=} \mathrm{E}\{\boldsymbol{n}_{\mathrm{o}}[k+\kappa]\boldsymbol{n}_{\mathrm{o}}^{\mathsf{H}}[k]\} = \sigma_n^2\,\boldsymbol{I}\,\delta[\kappa]$, with $\sigma_n^2 = \frac{N_0}{T}$ and $\delta[k]$ is the unit pulse sequence.

III. Equalization of MIMO ISI channels

In order to obtain decision symbols free of interference, from which by means of simple threshold decisions estimates of the data symbols can be obtained, the discrete-time processing at the transmitter has to be chosen suitably. Thereby, both intersymbol (temporal) and multiuser (spatial) interference have to be considered in common.

A very attractive equalization strategy is (nonlinear) *precoding* [16], [12], [6], initially introduced for single-input/singe-output ISI channels but immediately applicable to MIMO and MIMO ISI channels, e.g., [7]. Precoding can be derived from decision-feedback equalization (DFE), where already detected symbols assist in the equalization and detection of subsequent symbols. However, DFE is only applicable if the receive signals can be processed jointly, e.g., in an uplink scenario. Precoding can be seen as dual to DFE, where all receiver side processing is transfered to the transmitter. Using precoding, the boosting of average transmit power is avoided which would be present if linear (zero-forcing) pre-equalization via $\boldsymbol{F}(z) = \boldsymbol{H}_{\mathrm{o}}^{-1}(z)$ was applied.

The block diagram of Tomlinson-Harashima type precoding for MIMO ISI channels is shown in Fig. 2. Equalization is split between two matrix filter, the *feedforward filter* $\boldsymbol{F}(z)$ and the

This work has been supported in parts by Heinrich–Hertz–Institut für Nachrichtentechnik Berlin GmbH, Berlin.

[1]The same channel model is valid for a CDMA system, i.e., spreading codes are used for (incomplete) user separation rather than antennas.

[2]Notation: $\boldsymbol{A}^{\mathsf{T}}$: transpose of matrix $\boldsymbol{A}$; $\boldsymbol{A}^{\mathsf{H}}$: Hermitian (i.e., conjugate) transpose; $\boldsymbol{A}^{-\mathsf{H}}$: inverse of the Hermitian transpose of a square matrix $\boldsymbol{A}$. $\boldsymbol{I}$: Identity matrix. z^{-*} abbreviates $(z^{-1})^*$.

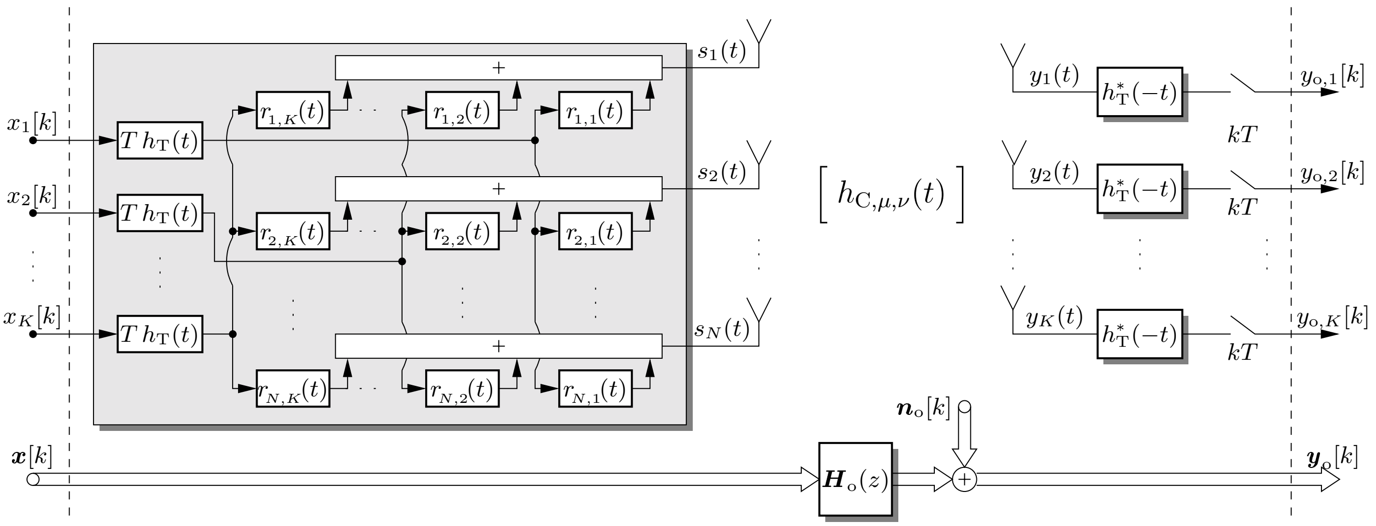

Fig. 1. Point-to-multipoint transmission over MIMO ISI channel and equivalent discrete-time model incorporating the matrix matched filter and T-spaced sampling. Abbreviation: $r_{\nu,\kappa}(t) = h^*_{\mathrm{C},\kappa,\nu}(-t)$.

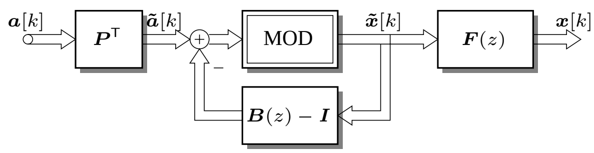

Fig. 2. Block diagram of Tomlinson-Harashima type precoding.

feedback filter $\boldsymbol{B}(z)$. The task of the feedforward filter is not to equalize the channel completely, but to shape the end-to-end signal transfer function $\boldsymbol{H}(z) = \sum_k \boldsymbol{H}_k\, z^{-k} \stackrel{\text{def}}{=} \boldsymbol{H}_{\mathrm{o}}(z)\boldsymbol{F}(z)$ to have some desired properties. This transfer function is then (nonlinearly) equalized by the feedback structure. For a zero-forcing (ZF) approach $\boldsymbol{B}(z) = \boldsymbol{H}(z)$. (The generalization to minimum mean-squared error (MMSE) precoding is not considered here.)

Assuming an M-ary square QAM constellation,[3] i.e., $a_\kappa \in \mathcal{A} = \left\{a_{\mathrm{I}} + \mathrm{j}a_{\mathrm{Q}} \mid a_{\mathrm{I}}, a_{\mathrm{Q}} \in \{\pm 1, \pm 3, \ldots, \pm(\sqrt{M}-1)\}\right\}$, the operation of the precoder is as follows: Given a suited permutation $\tilde{\boldsymbol{a}}[k]$ of the data symbols $a_\kappa[k]$ (performed by the permutation matrix $\boldsymbol{P}^{\mathsf{T}}$, see below) the intermediate symbols $\tilde{x}_\kappa[k]$ at time instant k are calculated successively as

$$\tilde{x}_1[k] = \tilde{a}_1[k] \qquad (2)$$

$$\begin{aligned} \tilde{x}_\kappa[k] &= \mathrm{MOD}\left\{\tilde{a}_\kappa[k] - f_\kappa[k]\right\} \\ &= \tilde{a}_\kappa[k] + d_\kappa[k] - f_\kappa[k]\,, \quad \kappa = 2, \ldots, K\,, \end{aligned} \qquad (3)$$

and $f_\kappa[k] = \sum_{l=1}^{\kappa-1} b_{\kappa l}[0]\tilde{x}_l[k] + \sum_{m>0}\sum_{l=1}^{K} b_{\kappa l}[m]\tilde{x}_l[k-m]$ is the sum of precursors over users and time. The precoding symbols $d_k \in \left\{2\sqrt{M}\cdot(d_{\mathrm{I}} + \mathrm{j}d_{\mathrm{Q}}) \mid d_{\mathrm{I}}, d_{\mathrm{Q}} \in \mathbb{Z}\right\}$ are chosen implicitly by the modulo device such that the real and imaginary part of the resulting symbol $\tilde{x}_k$ lie within the (half-open) interval $[-\sqrt{M}, \sqrt{M})$. These precoding symbols virtually extend the signal set $\mathcal{A}$ periodically; all points spaced by integer multiples of $2\sqrt{M}$ in real or imaginary part represent the same data. Symbol-by-symbol the best representative (smallest magnitude after the feedback loop) is chosen.

[3]The generalization to other signal sets is easily possible, see [6].

It can can be shown that the symbols $\tilde{x}_\kappa[k]$ at the output of the modulo device are (nearly) mutually and temporally uncorrelated and their variance is very well approximated by $\sigma^2_{\tilde{x}} = M/(M-1)\sigma^2_a$, i.e., only a slight increase in average transmit power compared to signaling using the data symbols $a_\kappa[k]$ is present.

For a successive processing of the symbols over space and time in the feedback loop, the feedforward filter should be chosen such that the following demands are met:

Causality: The end-to-end response should exhibit spatial and temporal causality, i.e., $\boldsymbol{H}_k = \boldsymbol{0}$, $k < 0$. Then, $\tilde{\boldsymbol{x}}[k]$ has only influence on subsequent time instances; future vectors $\tilde{\boldsymbol{x}}[\eta]$, $\eta < k$, have not to be considered when calculating $\tilde{\boldsymbol{x}}[k]$. Additionally, at each time instant k, symbols $\tilde{x}_m[k]$ should be generated successively, i.e., the symbols over space and time should be processed in a zig-zag fashion. For that, symbol $\tilde{x}_m[k]$ may only interfere into symbols $\tilde{x}_\kappa[k]$, $\kappa > m$. Hence, the zeroth coefficient of the end-to-end response, $\boldsymbol{H}_0$, has to be *lower triangular*.

Normalization: For unit-gain transmission of the users' signals, the zeroth coefficient of the end-to-end response, $\boldsymbol{H}_0$, should have a unit main diagonal. However, in order to fix total transmit power to the same level as the direct transmission of the data vectors $\boldsymbol{a}[k]$, $\boldsymbol{F}(z)$ has to be normalized suitably. This scaling is compensated at the receiver side by a gain factor g (automatic gain control), common to all receivers.

Minimum Phase Property and Processing Order: Since the decisions are based on the diagonal elements of the zeroth coefficient of the end-to-end response $\boldsymbol{H}(z)$ and all other terms are compensated via precoding (cf. the cancellation in DFE), these elements (before normalization) should be as large as possible. It can be shown, that optimum performance is achieved if $\boldsymbol{H}(z)$ is minimum phase, which for matrices is defined as $\det(\boldsymbol{H}(z))$ to have roots only inside the unit circle. Moreover, as the last degree of freedom, the processing order of the symbols has to be selected suitably. A permutation matrix $\boldsymbol{P}^{\mathsf{T}}$ can be introduced, which is chosen such that transmission over $\boldsymbol{P}^{\mathsf{T}}\boldsymbol{H}_{\mathrm{C}}(f)$ and detection in the natural ordering 1 through K gives the best performance. Since we are interested in precoding and the receivers can not cooperate, this permutation is done at the transmitter, too, see Figure 2.

IV. Spectral Factorization

For the above-mentioned demands, the optimum discrete-time feedforward matrix filter $\boldsymbol{F}(z)$ and the feedback matrix filter $\boldsymbol{B}(z)$ can be calculated given $\boldsymbol{H}_{\mathrm{o}}(\mathrm{e}^{\mathrm{j}2\pi fT})$ or its analytic continuation $\boldsymbol{H}_{\mathrm{o}}(z)$. This is done by performing a (spectral) factorization, which decomposes $\boldsymbol{H}_{\mathrm{o}}(z)$ according to [6]

$$\boldsymbol{P}^{\mathsf{T}}\boldsymbol{H}_{\mathrm{o}}(z)\boldsymbol{P} = \boldsymbol{S}(z)\cdot\boldsymbol{\Sigma}\cdot\boldsymbol{S}^{\mathsf{H}}(z^{-*}) \ . \tag{4}$$

Here, $\boldsymbol{P}$ is a permutation matrix (each row and column contains a single one, $\boldsymbol{P}\boldsymbol{P}^{\mathsf{T}} = \boldsymbol{I}$), $\boldsymbol{\Sigma} = \mathbf{diag}(\varsigma_1, \ldots, \varsigma_N)$ is real diagonal, and the matrix polynomial $\boldsymbol{S}(z) = \sum_{k\geq 0} \boldsymbol{S}_k\, z^{-k}$ is expected to be causal and minimum-phase ($\det(\boldsymbol{S}(z)) \neq 0$, $|z| \geq 1$). Moreover, $\boldsymbol{S}_0$ has to be lower triangular with unit main diagonal (“monic” matrix polynomial $\boldsymbol{S}(z)$).

From $\boldsymbol{S}(z)$ and $\boldsymbol{\Sigma}$, the feedforward filter calculates as

$$\boldsymbol{F}(z) = \boldsymbol{P}\,\boldsymbol{S}^{-\mathsf{H}}(z^{-*})\,\boldsymbol{\Sigma}^{-1}\,g^{-1} \ , \tag{5}$$

where the scaling factor g is chosen such that average transmit power is fixed (see above), which is often done, such that[4]

$$\int_{-1/2}^{+1/2} \mathrm{trace}\{\boldsymbol{F}(\mathrm{e}^{\mathrm{j}2\pi\phi})\boldsymbol{F}^{\mathsf{H}}(\mathrm{e}^{\mathrm{j}2\pi\phi})\}\ \mathrm{d}\phi = K \tag{6}$$

is valid. The requested causal, minimum-phase, and monic end-to-end transfer function reads

$$\boldsymbol{H}(z) = g\boldsymbol{H}_{\mathrm{o}}(z)\boldsymbol{F}(z) = \boldsymbol{P}\boldsymbol{S}(z) \ . \tag{7}$$

Since the additive noise $n_\kappa[k]$ is (temporally) white with variance σ_n^2, the signal-to-noise ratio (SNR) at each receiver reads $\mathrm{SNR}_\kappa = \sigma_a^2/(g^2\,\sigma_n^2)$, $\forall\kappa$.

In literature, a number of factorization algorithms for solving (4) are discussed, see, e.g., [13]. Among them, the one proposed in [18] seems to be of particular interest. This algorithm is an extension of the polynomial factorization via (repeated) Cholesky decomposition of a coefficient Toeplitz matrix introduced by F.L. Bauer in [1].

An easy-to-use iterative algorithm for the matrix factorization problem at hand can be derived if the optimal processing order is ignored in the first step. Hence, we first solve the modified factorization problem

$$\boldsymbol{H}_{\mathrm{o}}(z) = \boldsymbol{T}(z)\boldsymbol{T}^{\mathsf{H}}(z^{-*}) \ , \tag{8}$$

where $\boldsymbol{T}(z) = \sum_{k\geq 0} \boldsymbol{T}_k\, z^{-k}$, with $\boldsymbol{T}_0$ lower triangular and $\det(\boldsymbol{T}(z)) \neq 0$, $|z| > 1$, and $\boldsymbol{H}_{\mathrm{o}}(z) = \sum_k \boldsymbol{H}_{\mathrm{o},k}\, z^{-k}$. Similar to [1], (8) can be solved in an iterative way, see [9].

In the next step, the optimal processing order for minimal scaling factor g and hence maximum SNR is calculated. As explained above, here only the coefficient matrix at time index 0, i.e., $\boldsymbol{S}_0$ is of importance. Since, moreover, the spectral factorization is unique up to a unitary matrix, the optimal processing order can be derived based on the coefficient matrix $\boldsymbol{T}_0$ obtained from the above factorization. For that, we decompose $\boldsymbol{T}_0$ according to

$$\boldsymbol{P}^{\mathsf{T}}\cdot\boldsymbol{T}_0 = \boldsymbol{R}\cdot\boldsymbol{Q}^{\mathsf{H}} \ , \tag{9}$$

where $\boldsymbol{P}$ is the requested permutation matrix, $\boldsymbol{R} = [r_{l,m}]$ is lower triangular, and $\boldsymbol{Q}$ is a unitary matrix. This factorization can be performed by applying the V-BLAST algorithm[5] [11] to $\boldsymbol{T}_0^{\mathsf{H}}$.

Having performed the factorizations (8) and (9), we define $\boldsymbol{D} = \mathbf{diag}(r_{1,1}, \ldots, r_{K,K})$. Then, combining (4), (8), and (9), we can finally write the spectral factorization according to

$$\begin{aligned}\boldsymbol{P}^{\mathsf{T}}\boldsymbol{H}_{\mathrm{o}}(z)\boldsymbol{P} &= \boldsymbol{P}^{\mathsf{T}}\boldsymbol{T}(z)\boldsymbol{Q}\boldsymbol{D}^{-1}\boldsymbol{D}\,\boldsymbol{D}^{\mathsf{H}}\boldsymbol{D}^{-\mathsf{H}}\boldsymbol{Q}^{\mathsf{H}}\boldsymbol{T}^{\mathsf{H}}(z^{-*})\boldsymbol{P} \\ &= \boldsymbol{S}(z)\cdot\boldsymbol{\Sigma}\cdot\boldsymbol{S}^{\mathsf{H}}(z^{-*}) \ ,\end{aligned} \tag{10}$$

with $\boldsymbol{\Sigma} = \boldsymbol{D}^{\mathsf{H}}\boldsymbol{D}$, and $\boldsymbol{S}(z) = \boldsymbol{P}^{\mathsf{T}}\boldsymbol{T}(z)\boldsymbol{Q}\boldsymbol{D}^{-1}$. Due to construction and uniqueness of the factorization, this is the optimal solution to (4).

V. Simulation Results

In order to illustrate the performance of precoding for MIMO ISI channels and to show the advantage over linear preequalization numerical simulations were performed. Throughout this section we assume $N = 4$ antennas at the central transmitter and $K = 4$ decentralized receivers. Each user employs 16-QAM signaling. We assume a block-fading MIMO ISI channel which reflects a bursty transmission over a block-wise constant radio channel. The numerical results are averaged over a large number of channel realizations. In each case the channel is normalized such that the average energy of the MIMO ISI channel equals $N\cdot K$ and hence equals that of a one-tap (i.e., flat-fading) MIMO channel with the usual assumption of unit-energy fading coefficients. Moreover, the short-term transmit power is fixed; independent of the current channel realization, by normalization of the feedforward matrix $\boldsymbol{F}(z)$, the average transmit power is fixed to that of a direct transmission of the data symbols $a_\kappa[k]$.

First, a MIMO ISI channel with constant power-delay profile (pdp) (equal-gain test channel, T-spaced taps) is assumed. The elements of the tap matrices are chosen i.i.d. complex Gaussian with variance $1/L$. The length L of the impulse response of the underlying MIMO ISI channel is selected as $L = 2$, 4, and 8. Figure 3 shows the symbol error rate (SER) over the ratio of total average transmitted energy per information bit $\bar{E}_{\mathrm{b}}$ and one-sided noise power spectral density N_0 of the channel. Three cases are considered: linear preequalization, precoding without optimized processing order, and precoding employing the optimal processing order as described above.

[4]Note, this normalization does not necessarily result in a fixed short-term average transmit power since for actual power calculation the transmit filters $H_{\mathrm{T}}(f)$ and the channel matched filters $\boldsymbol{H}_{\mathrm{C}}^{\mathsf{H}}(f)$ have to be taken into into account. To be precise, power normalization has to be done with respect to $\boldsymbol{H}_{\mathrm{C}}^{\mathsf{H}}(f)\,H_{\mathrm{T}}(f)\,\boldsymbol{F}(\mathrm{e}^{\mathrm{j}2\pi fT})$. When starting from a discrete-time channel model $\boldsymbol{H}_{\mathrm{C}}(z)$, power normalization is done with respect to $\boldsymbol{H}_{\mathrm{C}}^{\mathsf{H}}(\mathrm{e}^{\mathrm{j}2\pi\phi})\boldsymbol{F}(\mathrm{e}^{\mathrm{j}2\pi\phi})$. This type of normalization is used for the numerical results in this paper.

[5]The V-BLAST algorithm can be described to perform a sorted QR-type decomposition of a matrix $\boldsymbol{H}$ according to $\boldsymbol{H}\boldsymbol{P} = \boldsymbol{Q}^{\mathsf{H}}\boldsymbol{S}$, with permutation matrix (optimal sorting) $\boldsymbol{P}$, unitary matrix $\boldsymbol{Q}$, and lower triangular matrix $\boldsymbol{S}$. It can be shown, that the sorting criteria of V-BLAST also leads to the (almost) optimum solution for the present situation. Defining the anti-diagonal identity matrix $\boldsymbol{J} = [j_{l,m}]$, $j_{l,N+1-l} = 1$, zero else, with $\boldsymbol{J}^2 = \boldsymbol{I}$, we can write the decomposition problem (9) as $\boldsymbol{T}_0^{\mathsf{H}}\boldsymbol{P}\boldsymbol{J} = \boldsymbol{Q}\boldsymbol{J}\,\boldsymbol{J}\boldsymbol{R}^{\mathsf{H}}\boldsymbol{J} = \boldsymbol{Q}'\boldsymbol{R}'$. Applying the V-BLAST algorithm results in $\boldsymbol{P}' = \boldsymbol{P}\boldsymbol{J}$, $\boldsymbol{Q}' = \boldsymbol{Q}\boldsymbol{J}$, and $\boldsymbol{R}' = \boldsymbol{J}\boldsymbol{R}^{\mathsf{H}}\boldsymbol{J}$, from which the requested matrices are immediately obtained.

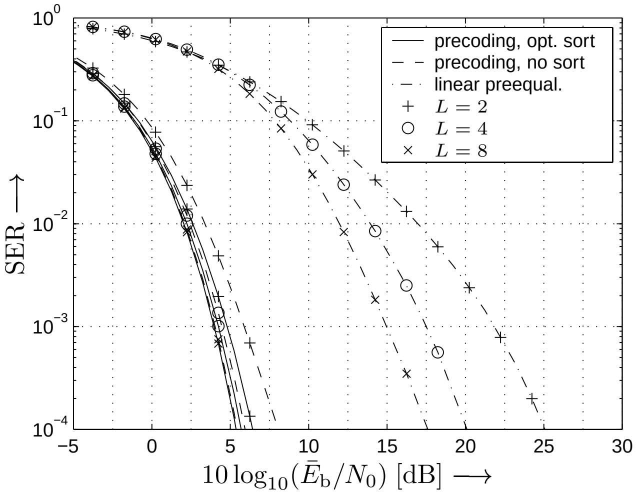

Fig. 3. Symbol error rate over signal-to-noise $\bar{E}_\mathrm{b}/N_0$ (in dB) for linear preequalization and precoding using an arbitrary processing order and the optimal processing order. $N = 4$ transmit antennas, $K = 4$ users, 16-QAM modulation. Constant power-delay profile with $L = 2$, 4, and 8 T-spaced taps; i.i.d. complex Gaussian elements of the tap matrices.

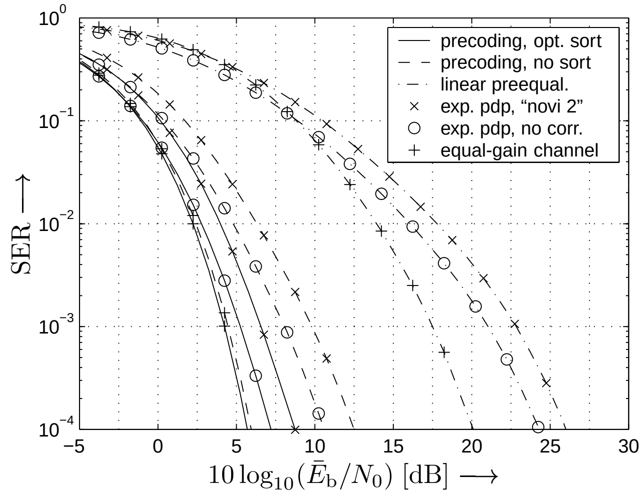

Fig. 4. Symbol error rate over signal-to-noise $\bar{E}_\mathrm{b}/N_0$ (in dB) for linear preequalization and precoding using an arbitrary processing order and the optimal processing order. $N = 4$ transmit antennas, $K = 4$ users, 16-QAM modulation. Exponentially decaying power-delay profile; correlation of the complex Gaussian elements of the tap matrices according to the scenario "novi 2" [15] ($\times$); no correlations ($\circ$). For comparison: constant power-delay profile, no correlations ($+$).

In each case precoding significantly outperforms linear preequalization. Moreover, the advantage of temporal diversity is visible. Increasing the length of the impulse response, the performance gets better and the gain of precoding over linear preequalization decreases. At the same time, the differences between the error rates for precoding using an arbitrary processing order and using the optimal processing order almost vanish. If a sufficient degree of diversity is available, the elements ς_κ of $\mathbf{\Sigma}$ in (4) become very similar, and in turn sorting is of minor importance.

This fact is supported by the results shown in Figure 4, where for $L = 4$ an exponentially decaying power-delay profile, borrowed from the "Pedestrian A" power-delay profile, cf. [17], is assumed (lines marked with circles). The taps are again i.i.d. complex Gaussian. Since this channel does not provide as much diversity as the equal-gain channel with $L = 4$ (shown for reference; lines marked with "$+$"), the slope of the curves is somewhat smaller. Moreover, for the present case, sorting is much more significant as for a constant power-delay profile.

Finally, we consider the statistical MIMO radio channel model proposed in [14]. The power-delay profile is exponentially decaying (the same as used above) and spatial correlations of the transmit antennas are present. Due to the decentralized receivers in the present broadcast scenario the received signals are assumed to be spatially uncorrelated, i.e., among the correlation matrices provided by [15] only the transmitter (base station) parameters are employed. In particular, correlated transmit antennas according to the scenario "novi 2" [15] with an impulse response of length $L = 4$ is used. From Figure 4, a loss of about 2 dB due to spatial correlations is observable. Only with very small probability the present correlations results in channel realizations with rank deficit which, in turn, would lead to very poor performance. However, as for the channel with exponentially decaying power-delay profile without correlations, the use of the optimal processing order is advisable.

References

[1] F.L. Bauer. Ein direktes Iterationsverfahren zur Hurwitz–Zerlegung eines Polynoms. *Intern. Journal of Electr. and Comm.*, pp. 285–290, 1955.

[2] G. Caire, S. Shamai. On the Achievable Throughput of a Multiantenna Gaussian Broadcast Channel. *IEEE Tr. IT*, pp. 1691–1706, July 2003.

[3] T. Ericson. Structure of Optimum Receiving Filters in Data Transmission Systems. *IEEE Tr. IT*, pp. 352–353, May 1971.

[4] W. Van Etten. An Optimum Linear Receiver for Multiple Channel Digital Transmission Systems. *IEEE Tr. COM*, pp. 828–834, Aug. 1975.

[5] W. Van Etten. Maximum Likelihood Receiver for Multiple Channel Transmission Systems. *IEEE Tr. COM.*, pp. 276–283, Feb. 1976.

[6] R.F.H. Fischer. *Precoding and Signal Shaping for Digital Transmission*. John Wiley & Sons, Inc., New York, 2002.

[7] R.F.H. Fischer, C. Windpassinger, A. Lampe, J.B. Huber. Space-Time Transmission using Tomlinson-Harashima Precoding. *4th International ITG Conference on Source and Channel Coding*, Berlin, Jan. 2002.

[8] R.F.H. Fischer, C. Windpassinger, A. Lampe, J.B. Huber. MIMO Precoding for Decentralized Receivers. *IEEE Intern. Symp. on Inf. Theory*, p. 496, Lausanne, Switzerland, June/July 2002.

[9] R.F.H. Fischer, J.B. Huber. Signal Processing in Receivers for Communication over MIMO ISI Channels. *IEEE Intern. Symp. on Signal Proc. and Inform. Techn.*, Darmstadt, Germany, Dec. 2003.

[10] G. Ginis and J.M. Cioffi, Vectored-DMT: A FEXT canceling modulation scheme for coordinating users. *Intern. Conf. on Comm.*, Helsinki, Finland, June 2001.

[11] G.D. Golden, G.J. Foschini, R.A. Valenzuela, P.W. Wolniansky. Detection algorithm and initial laboratory results using V-BLAST space-time communication architecture. *Electronics Letters*, pp. 14–15, Jan. 1999.

[12] H. Harashima, H. Miyakawa. Matched-transmission technique for channels with intersymbol interference, *IEEE Tr. COM*, pp. 774–780, Aug. 1972.

[13] V. Kučera. Factorization of Rational Matrices: A Survey of Methods. *IEE Intern. Conf. on Control*, pp. 1074–1078, Edinburgh, 1991.

[14] K.I. Pedersen, J.B. Andersen, J.P. Kermoal, P.E. Mogensen. A Stochastic Multiple-Input-Multiple-Output Radio Channel Model for Evaluation of Space-Time Coding Algorithms. *IEEE Vehicular Techn. Conf.*, pp. 893-897, Boston, Sep. 2000.

[15] L. Schumacher, J.P. Kermoal, F. Frederiksen, K.I. Pedersen, A. Algans P.E. Mogensen. MIMO Channel Characterisation. *IST Project IST–1999–11729 METRA Deliverable 2*, Feb. 2001.

[16] M. Tomlinson. New automatic equaliser employing modulo arithmetic, *Electronics Letters*, pp. 138–139, March 1971.

[17] ETSI. *Selection Procedures for the Choice of Radio Transmission Technologies of the UMTS (UMTS 30.03 version 3.2.0)*, 1998.

[18] D.C. Youla, N.N. Kazanjian. Bauer-Type Factorization of Positive Matrices and the Theory of Matrix Polynomials Orthogonal on the Unit Circle, *IEEE Tr. CS*, pp. 57–69, Feb. 1978.